

# Crystal Structure of the Product of $\text{Mg}^{2+}$ Insertion into $\text{V}_2\text{O}_5$ Single Crystals

V. Shklover<sup>1</sup> and T. Haibach

*Laboratory of Crystallography, Swiss Federal Institute of Technology, CH-8092 Zürich, Switzerland*

F. Ried

*Institute of Mineralogy and Petrography, Swiss Federal Institute of Technology, CH-8092 Zürich, Switzerland*

R. Nesper

*Laboratory of Inorganic Chemistry, Swiss Federal Institute of Technology, CH-8092 Zürich, Switzerland*

and

P. Novák

*Paul Scherrer Institute, Electrochemistry Section, CH-5232 Villigen PSI, Switzerland*

Received May 10, 1995; in revised form December 12, 1995; accepted February 15, 1996

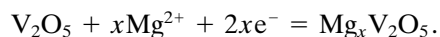
Chemical (by interaction with a dibutylmagnesium solution) and electrochemical (in acetonitrile solution of magnesium perchlorate) insertion of  $\text{Mg}^{2+}$  into the single crystals of  $\text{V}_2\text{O}_5$  was performed. The morphology change of  $\text{V}_2\text{O}_5$  crystals as a result of the  $\text{Mg}^{2+}$  insertion was studied by scanning electron microscopy. The wavelength dispersive electron probe microanalysis clearly showed the presence of Mg (at least) at the surface of intercalated  $\text{V}_2\text{O}_5$ . Based on the single crystal X-ray diffraction study of intercalated  $\text{V}_2\text{O}_5$  (orthorhombic,  $Pmn2_1$ ,  $a = 11.544(6)$ ,  $b = 4.383(3)$ ,  $c = 3.574(2)$  Å,  $Z = 4$ ) the location of a small amount of Mg (~1%) in the bulk  $\text{V}_2\text{O}_5$  may be suggested, with [6 + 4] oxygen atoms surrounding Mg. The resulting Mg–O separations essentially exceed the accepted values for the Mg–O distances in crystals with hexacoordinated Mg atoms, which may be correlated with the structural and electrochemical properties of  $\text{Mg}^{2+}$ -inserted  $\text{V}_2\text{O}_5$ . © 1996 Academic Press, Inc.

## INTRODUCTION

Vanadium pentoxide,  $\text{V}_2\text{O}_5$ , is one of the electroactive materials suitable for the positive insertion electrode of a secondary magnesium battery (1, 2).  $\text{Mg}^{2+}$  ions can be inserted into the oxide chemically or electrochemically.

<sup>1</sup> To whom correspondence should be addressed.

An overall scheme for the electrochemical reaction can be written as



In the previous structural study (3) we have concentrated on the polycrystalline products of chemical and electrochemical  $\text{Mg}^{2+}$  insertion in  $\text{V}_2\text{O}_5$  and related Na- and Mg-vanadium bronzes,  $\text{Na}_2\text{V}_6\text{O}_{16}$  and  $\text{MgV}_6\text{O}_{16}$ . These bronzes were prepared with the intention to increase the distances between the layers in the  $\text{V}_2\text{O}_5$  lattice by inserting Na or Mg and, thus, to facilitate the subsequent insertion of excess  $\text{Mg}^{2+}$  ions. We have shown that (a) the chemical and electrochemical  $\text{Mg}^{2+}$  insertion in  $\text{V}_2\text{O}_5$  produces similar  $\text{V}_2\text{O}_5$ -related phases, (b) the product of the reversible electrochemical reduction of  $\text{V}_2\text{O}_5$  in wet acetonitrile containing  $\text{Mg}(\text{ClO}_4)_2$  has multiphase character, (c) the content in the electrode of one of the new phases decreases during an electrochemical cycling, and (d) two layered phases coexist in the hydrated sodium vanadium bronzes,  $\text{Na}_2\text{V}_6\text{O}_{16}(\text{H}_2\text{O})_y$ , one of which (with  $y = 3$ ) is the electrochemically most active and allows  $\text{Mg}^{2+}$  insertion to a higher extent. All products of the  $\text{Mg}^{2+}$  insertion in  $\text{V}_2\text{O}_5$  and related vanadium bronzes described in (3) are poorly crystalline and allow only for limited correlations of structural changes with the chemical or electrochemical treatment. The wavelength dispersive electron probe micro-

analysis (EPMA) was used in (3) for the determination of the Mg content, which has been found to be equal to 11.7–12.2 at% in the product of the direct chemical  $\text{Mg}^{2+}$  insertion into the bronze  $\text{Na}_2\text{V}_6\text{O}_{16}(\text{H}_2\text{O})_3$ , 1.0–1.2 at% in the product of chemical  $\text{Mg}^{2+}$  insertion in the polycrystalline  $\text{V}_2\text{O}_5$ , 0.14 at% and 1.3–1.5 at% in the yellow and brown microcrystalline products of chemically prepared bronzes  $\text{Mg}(\text{V}_3\text{O}_8)_2(\text{H}_2\text{O})_y$ . The product of subsequent chemical  $\text{Mg}^{2+}$  insertion into the last bronzes contained 3.8–4.0 at% Mg.

Structure investigations of products of  $\text{Mg}^{2+}$  insertion into the  $\text{V}_2\text{O}_5$  single crystal are also important because they could allow a direct determination of the coordination of inserted Mg atoms in the lattice of the host  $\text{V}_2\text{O}_5$  single crystal. This paper summarizes our work on this topic.

### SYNTHESIS

The  $\text{V}_2\text{O}_5$  single crystals, a gift of Professor K. Kato of the National Institute for Research in Inorganic Materials, Tsukuba, Japan, were prepared by Y. Uchida and E. Bannai from reagent grade  $\text{V}_2\text{O}_5$  of 99.99% purity using the floating-zone technique in an image furnace (4). The as-received, long crystals were cut with a stainless steel blade into small pieces (less than ca.  $1 \times 1 \times 0.2$  mm) before being used in the experiments. To avoid oxygen and moisture contamination, all manipulations were performed in an Ar-filled glove box in which the  $\text{H}_2\text{O}$  and  $\text{O}_2$  levels were not permitted to exceed 5 ppm. The measurements were performed in hermetically sealed containers assembled in the glove box.

Chemical insertion experiments involved placing the  $\text{V}_2\text{O}_5$  single crystals in contact with excess ( $\sim 10$  cm<sup>3</sup>) of 1.0 M dibutylmagnesium solution in heptane (Aldrich 34,511-3; a 1:1 mixture of *n*- and *sec*-butyl groups), and allowing them to react under occasional shaking (several times a week) at 25°C for 2 months. The crystals were then rinsed with dry heptane (Aldrich) several times during a period of a few days, dried in the glove box atmosphere overnight, and sealed under Ar.

The electrochemical insertion of  $\text{Mg}^{2+}$  in the  $\text{V}_2\text{O}_5$  single crystals was performed at 25°C in an acetonitrile solution containing 1 M  $\text{Mg}(\text{ClO}_4)_2$  and 0.9 M  $\text{H}_2\text{O}$ . Electrochemical cells with working and counter electrodes pressed together with a spring ( $\sim 2$  kg · cm<sup>-2</sup>) but separated by an electrolyte-soaked glass-fiber separator were employed. The contact of the single crystals with a glassy carbon current collector in this spring-loaded cell was obtained by the permanent mechanical pressure in the cell. A magnesium counterelectrode and an Ag/Ag<sup>+</sup> reference were used. In the experiments, the electrode potential was initially swepted at 0.5 μV/s from its open circuit value to -1.4 V vs Ag/Ag<sup>+</sup>. Then, the single crystals were reduced at -1.4 V for 5 weeks. During this procedure, the orange-

yellow color of the  $\text{V}_2\text{O}_5$  turned dark. The reduced crystals were washed with dry deoxygenated acetonitrile overnight, dried in the glove box atmosphere, and sealed hermetically under Ar.

### X-RAY SINGLE CRYSTAL STUDY

After the chemical  $\text{Mg}^{2+}$  insertion the crystals of  $\text{V}_2\text{O}_5$  lost their single crystal character and were not suitable for X-ray single crystal investigations anymore. But one of the crystals (I) subjected to the electrochemical  $\text{Mg}^{2+}$  insertion was still good enough for a single crystal X-ray analysis in spite of the splitting of the diffraction peaks. The partial destruction of the crystal has been observed in an optical microscope, as well.

Diffraction data on crystal I were collected at 293 K on the Nicolet R3 four-circle diffractometer using  $\text{MoK}\alpha$  radiation with a graphite monochromator. The lattice parameters were refined with 24 centered reflections with  $2\theta$  values between 22° and 24°. The  $\omega/2\theta$  scan technique to  $2\theta_{\text{max}} = 60^\circ$  was used to record the intensities of 296 reflections. The coordinates of V and O atoms were found by direct methods using the TREF procedure. The absorption correction for the real form of the crystal using 8 reflections was introduced during the refinement (maximum and minimum transmissions are 0.075 and 0.019) and decreased the *R* value from 0.2147 to 0.1295. After the anisotropic refinement of V and O atoms to *R* = 0.081 (the parallel refinement of V and O atoms in the centrosymmetric space group *Pmnm* gave considerably larger value of *R* = 0.095), the difference Fourier synthesis was calculated. One of the strongest peaks, at the distances to O atoms of about 2.4–2.6 Å, was assigned to Mg (Mg(1)). The refinement of structure I with the Mg(1) atom at this position with an occupation factor of 1.0 did not bring its isotropic temperature factor to a high value. At the fixed value of temperature factor of Mg(1) taken from the previous isotropic refinement, the occupation factor for supposed Mg(1) was refined together with its positional parameters and equals 0.01(3). The final values of residuals were *R* = 0.076 (*R*<sub>w</sub> = 0.073).

The data collection of the native single crystal  $\text{V}_2\text{O}_5$  (II) was performed at 293 K on an Enraf-Nonius CAD-4 diffractometer using  $\text{MoK}\alpha$  radiation ( $\lambda = 0.71073$  Å) equipped with a graphite monochromator. Using an  $\omega/2\theta$  scan technique all reflections in the range  $2.92^\circ < 2\theta < 30.44^\circ$  were collected using the CAD4-EXPRESS software (5). The index ranges were  $-3 < h < 0$ ,  $0 < k < 4$ ,  $-11 < l < 0$ . Three standard reflections were measured every 1 h for the intensity control and two standard reflections were checked every 100 reflections for the orientation control. The intensities were measured with a prescan determined scan speed to reach the ration  $\sigma(I)/I = 0.03$ , the maximum measurement time was 1 min per reflection. For

TABLE 1  
Experimental Details of X-Ray Determination of the Structures I, IIa, and IIb

	I	IIa (IIb)		I	IIa (IIb)
Empirical formula	Mg <sub>0.01</sub> V <sub>2</sub> O <sub>5</sub>	V <sub>2</sub> O <sub>5</sub>	Scan mode	$\omega/2\theta$	$\omega/2\theta$
Crystal size (mm)	0.2 × 0.4 × 0.05	0.3 × 0.5 × 0.03	Reflections collected	296	483
Crystal system	Orthorhombic	Orthorhombic	$R_{\text{int}}$	0.060	0.037
Space group	<i>Pmn</i> 2 <sub>1</sub>	<i>Pmn</i> 2 <sub>1</sub> ( <i>Pmnn</i> )	Independent reflections	296	
Lattice parameters			Observed reflections		
<i>a</i> (Å)	11.544(6)	11.544(2)	( $I > 2.0\sigma(I)$ )	259	380
			Reflections in refinement	254	374
<i>b</i> (Å)	4.383(3)	4.383(1) (3.571(1))	Refinement method	Full-matrix	
<i>c</i> (Å)	3.574(2)	3.571(1) (4.383(1))		least-squares	
<i>V</i> (Å <sup>3</sup> )	180.8(2)	180.7(1)	Function minimized	$\sum w(F_o - F_c)^2$	
<i>Z</i>	2	2	Weighting scheme	$w = (\sigma^2(F) + kF^2)^{-1}$	
Formula weight	182.14	181.87 (90.94)	<i>k</i>	0.0111	0.0074 (0.0072)
Density (calc, Mg.m <sup>-3</sup> )	3.365	3.362	Number of parameters	36	33 (23)
Absorption coefficient (mm <sup>-1</sup> )	3.85 <sup>a</sup>	3.76	Residuals <i>R</i>	0.0763	0.0436 (0.0434)
<i>F</i> (000)	129.0 <sup>a</sup>	117.0	$R_w$	0.0735	0.0416 (0.0427)
Radiation	MoK $\alpha$	MoK $\alpha$	Reflection/parameter	7.1 : 1	11.3 : 1 (16.3 : 1)
$\lambda$	0.71069 Å	0.71073	Goodness of fit	0.93	0.64 (0.070)
Monochromator	Graphite	Graphite	Largest difference peak (e.Å <sup>-3</sup> )	1.79	1.68 (1.73)
Data collection at (K)	293	293	Largest difference hole (e.Å <sup>-3</sup> )	-1.59	-1.59 (-1.59)
2 $\theta$ range (degr.)	2.0–30.0	2.92–30.44			

<sup>a</sup> For Mg<sub>x</sub>V<sub>2</sub>O<sub>5</sub>, when  $x = 0.5$ .

the absorption correction, the  $\psi$ -scans of 9 reflections with the step  $\Delta\psi = 10^\circ$  were performed. The minimum and maximum transmissions were 0.64 and 0.99, respectively. The mean value of the  $|E^2 - 1|$  (0.910, XPREP program) was closer to the one expected for centrosymmetrical structure (0.968), as to the noncentrosymmetric one (0.736). Nevertheless, the parallel refinement of crystal structure II in noncentrosymmetric and centrosymmetric space groups *Pmn*2<sub>1</sub> (structure IIa) and *Pmnn* (structure IIb) was performed. The residual values ( $R = 0.0436$ ,  $R_w = 0.0416$  for IIa and  $R = 0.0434$ ,  $R_w = 0.0427$  for IIb) are very similar.

The crystallographic data of crystals I and II are given in Table 1, the positional and equivalent isotropic parameters are listed in Tables 2–4. The anisotropic displacement parameters of anisotropically refined atoms and a list of the observed and calculated structure factors have been submitted as supplementary material.<sup>2</sup> The bond lengths and angles in structure I are collected in Table 5. All calculations were performed on a VAX 3100 station using the SHELXTL-PLUS program package (6).

#### WAVELENGTH DISPERSIVE ELECTRON PROBE MICROANALYSIS

The chemical composition of a single crystal V<sub>2</sub>O<sub>5</sub> after electrochemical Mg-insertion was analyzed by electron microprobe analysis (EPMA) with a Cameca SX50. One of

the V<sub>2</sub>O<sub>5</sub> single crystals (treated under the same conditions as crystal I), with the dimensions 0.4 × 0.2 × 0.05 mm, was glued to the sample holder with a conducting carbon film and covered with a 20 nm carbon layer. The electron probe microanalyzer Cameca SX50 consists of five spectrometers, which allows the simultaneous analysis of five elements. The electron beam conditions were 15 kV acceleration voltage at 20 nA beam current for an optimum excitation of the analyzed X-ray lines of V and Mg. The VK $\alpha_1$  was detected at 2.5, MgK $\alpha_1$  at 9.9 Å with PET and TAP monochromator crystals, respectively, and reference samples were V metal and MgO periclase for V and Mg, respectively. The dimensions of the analyzed volume were

TABLE 2  
Atomic Coordinates ( $\times 10^4$ ) and Equivalent Isotropic Displacement Coefficients (Å<sup>2</sup>,  $\times 10^3$ )<sup>a</sup> in Structure I

	<i>x</i>	<i>y</i>	<i>z</i>	<i>U</i> (eq) <sup>a</sup>
V(1)	1487(1)	3924(3)	0	14(1)
Mg(1)	1/2	767(518)	-12(681)	32(49)
O(1)	1461(4)	324(16)	-9(42)	24(2)
O(2)	3193(4)	5056(15)	-32(27)	18(2)
O(3)	0	5017(20)	-33(56)	18(2)

<sup>a</sup> Equivalent isotropic *U* defined as one third of the trace of the orthogonalized  $U_{ij}$  tensor.

TABLE 3  
Atomic Coordinates ( $\times 10^4$ ) and Equivalent Isotropic Displacement Coefficients ( $\text{\AA}^2$ ,  $\times 10^4$ )<sup>a</sup> in Structure IIa

	x	y	z	$U(\text{eq})^a$
V(1)	1487.8(0.3)	3913(1)	0	75(2)
O(1)	1457(2)	303(7)	295(37)	141(10)
O(2)	3191(2)	5027(5)	49(30)	95(5)
O(3)	0	4995(8)	25(9)	127(9)

<sup>a</sup> Equivalent isotropic  $U$  defined as one third of the trace of the orthogonalized  $U_{ij}$  tensor.

approximately 2  $\mu\text{m}$  in diameter and 3–4  $\mu\text{m}$  in depth. Acquisition time on the peak was 10 sec for each element. Background intensities were measured with a symmetrical offset on both sides of the peak for a 10 sec total time and were subtracted from the peak intensities. After the correction for dead-time of the gas-flow counter, they were compared to the intensities of the reference sample to yield an initial concentration. The data were corrected for the matrix effects using the ZAF-correction. The concentration of MgO varied from 0.389 to 0.521 wt%, or  $x = 0.017$  to 0.021 for the  $(\text{V}_2\text{O}_5)_{1-x}(\text{MgO})_x$ . The minimum detectable limit was at 0.09 wt% for a single analysis.

### SCANNING ELECTRON MICROSCOPY

The single crystals of  $\text{Mg}^{2+}$ -inserted  $\text{V}_2\text{O}_5$  were examined at 30 kV accelerating voltage in a Hitachi S-900 "in-lens" field-emission scanning electron microscope with a standard Everhard-Thornley SE detector and YAG-type BSE detector. The Digital Micrograph 2.1 software was used for the digital processing of SEM images (7).

### DISCUSSION

The SEM micrographs show a very characteristic rough morphology of the  $\text{V}_2\text{O}_5$  single crystals after the electrochemical  $\text{Mg}^{2+}$  intercalation (Fig. 1). The observed conservation of the initial yellow color in the bulk of the  $\text{Mg}^{2+}$ -

TABLE 4  
Atomic Coordinates ( $\times 10^4$ ) and Equivalent Isotropic Displacement Coefficients ( $\text{\AA}^2$ ,  $\times 10^4$ )<sup>a</sup> in Structure IIb

	x	y	z	$U(\text{eq})^a$
V(1)	6012.3(0.3)	1/4	1086(1)	75(2)
O(1)	4309(2)	1/4	-28(5)	99(5)
O(2)	6045(2)	1/4	4697(7)	174(7)
O(3)	3/4	1/4	8(8)	127(8)

<sup>a</sup> Equivalent isotropic  $U$  defined as one third of the trace of the orthogonalized  $U_{ij}$  tensor.

TABLE 5  
The Relevant Interatomic Distances ( $\text{\AA}$ ) and Bond Angles (degr.)<sup>a</sup> in Structure I

V(1)–O(1)	1.578(7)	V(1)–O(2)	2.031(5)
V(1)–O(2a)	1.868(5)	V(1)–O(2b)	1.889(5)
V(1)–O(3)	1.782(3)	V(1) $\cdots$ O(1a)	2.805(7)
O(1)V(1)O(2)	105.2(2)	O(1V(1)O(2a)	103.8(6)
O(1)V(1)O(2b)	104.2(6)	O(1)V(1)O(3)	104.5(3)
O(1a)V(1)O(2)	76.5(2)	O(1a)V(1)O(2a)	76.4(4)
O(1a)V(1)O(2b)	76.3(4)	O(1a)V(1)O(3)	73.8(3)
O(2)V(1)O(2a)	75.4(4)	O(2)V(1)O(2b)	75.8(3)
O(2a)V(1)O(3)	96.8(6)	O(2b)V(1)O(3)	97.6(6)
O(2)V(1)O(3)	150.3(3)	O(2a)V(1)O(2b)	144.1(4)
O(1)V(1)O(1a)	178.3(4)		
Mg(1)–O(1) $\times 4^b$	2.50(18)	Mg(1)–O(3) $\times 2^c$	2.57(24)
Mg(1) $\cdots$ O(2d)	2.81(16)	Mg(1) $\cdots$ O(2a)	3.26(17)
Mg(1) $\cdots$ O(3) $\times 2^d$	3.10(23)		
O(1b)Mg(1)O(1c)	91.1(17)	O(1b)Mg(1)O(1d)	84.7(70)
O(1b)Mg(1)O(1e)	180.1(99)	O(1b)Mg(1)O(3a)	69.0(55)
O(1b)Mg(1)O(3c)	129.4(61)	O(1c)Mg(1)O(3a)	129.2(6)
O(1c)Mg(1)O(3c)	68.9(60)	O(3a)Mg(1)O(3c)	170.9(97)

<sup>a</sup> Symmetry equivalent atoms bonded to unique atoms: O(1a) (0.1461, 1.0324, -0.0009), O(1b) (0.3539, -0.0324, 0.4991), O(1c) (0.3539, -0.0324, -0.5009), O(1d) (0.6461, -0.0324, 0.4991), O(1e) (0.6461, -0.0324, -0.5009), O(2a) (0.1807, 0.4944, 0.4968), O(2b) (0.1807, 0.4944, -0.5032), O(2d) (0.6807, 0.5056, -0.0032), O(3a) (1/2, 0.4983, 0.4967), O(3b) (1/2, -0.5017, 0.4967), O(3c) (1/2, 0.4983, -0.5033), O(3d) (1/2, -0.5017, -0.5033).

<sup>b</sup> O(1a), O(1b), O(1c), and O(1d).

<sup>c</sup> O(3a) and O(3c).

<sup>d</sup> O(3b) and O(3d).

intercalated  $\text{V}_2\text{O}_5$  crystals indicate an incomplete diffusion of  $\text{Mg}^{2+}$  ions into the bulk of the  $\text{V}_2\text{O}_5$  single crystals under the applied conditions of electrochemical reduction. The prevailing mechanism of the solid state insertion reaction seems to prevent the achievement of a high degree of topochemically controlled bulk conversion and proceeds with surface processes and preferred reactions on the imperfections of the initial single crystal; see, e.g., (8, 9). The location of  $\text{Mg}^{2+}$  mainly on the surface of crystal I is deduced from the EPMA results. It is probable that this type of reaction may strongly hinder the rate and the speed of the bulk intercalation with the formation of surface layers of, e.g., products of irreversible reactions (e.g., formation of MgO). The topochemical intercalation of  $\text{Mg}^{2+}$  into the  $\text{V}_2\text{O}_5$  single crystal is obviously electrostatically retarded due to the double charge of  $\text{Mg}^{2+}$  ion. The size of the ion  $\text{Mg}^{2+}$  seems not to be a relevant parameter because the topochemical insertion of  $\text{Li}^+$ , with approximately the same ionic size, proceeds to a large extent (10).

In the bulk of  $\text{V}_2\text{O}_5$  the suggested Mg(1) atoms occupy positions on the mirror planes between the layers of V atoms (Fig. 2). Of course, the low accuracy of the found Mg–O separations in structure I does not allow one to

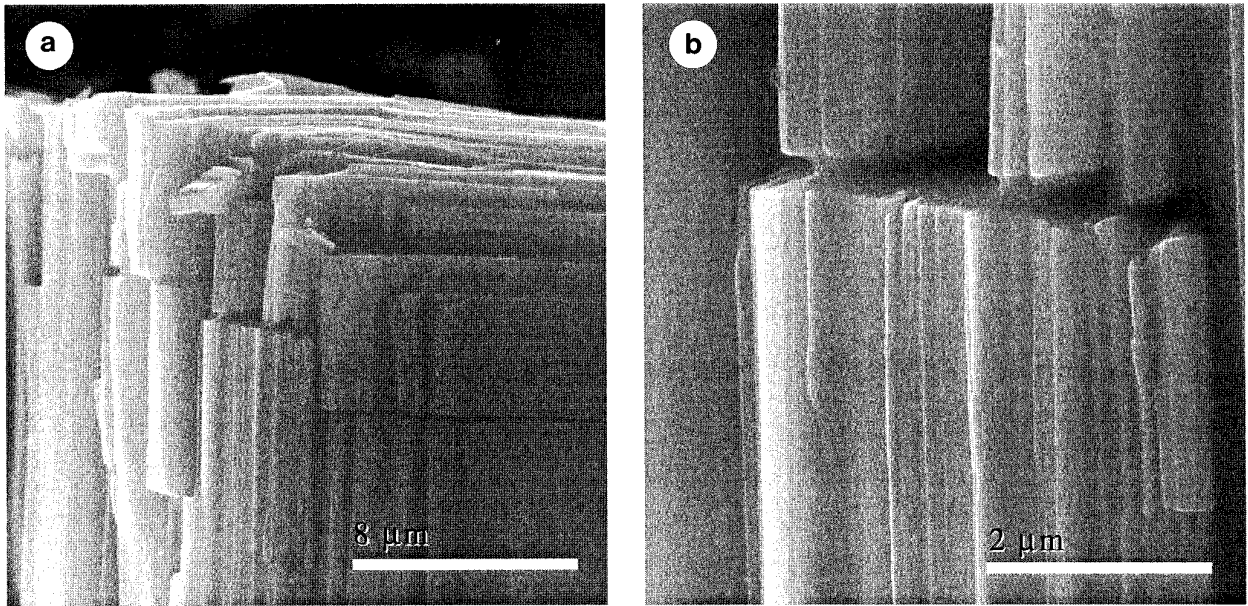


FIG. 1. SEM micrographs of V<sub>2</sub>O<sub>5</sub> single crystal after the electrochemical Mg<sup>2+</sup> insertion. The micrographs were taken approximately parallel (a) and perpendicular (b) to the plane *ac* of crystal I.

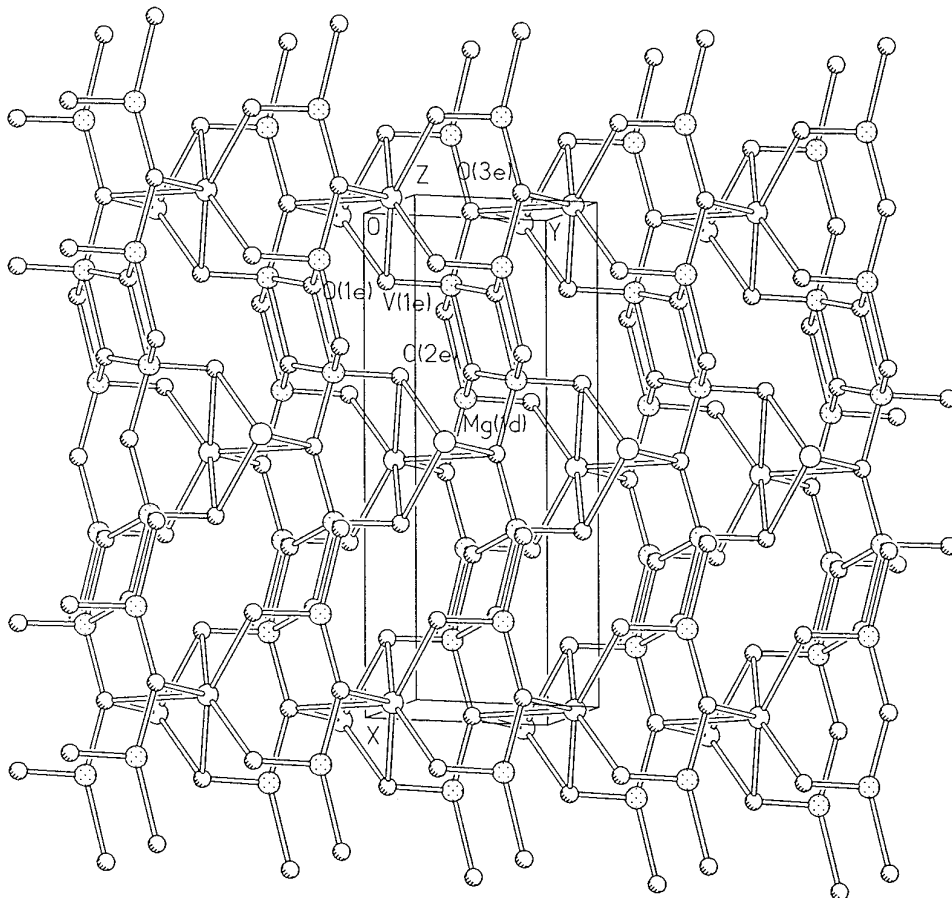


FIG. 2. Projection of crystal structure I on the plane *ab*. For the designations of the symmetry-related atoms see Table 4.

TABLE 6  
Comparison of Structural Parameters of I with Structurally Studied Mg Vanadates

	I	MgVO <sub>3</sub>	MgV <sub>2</sub> O <sub>6</sub>	Mg <sub>2</sub> V <sub>2</sub> O <sub>7</sub>	Mg <sub>3</sub> (VO <sub>4</sub> ) <sub>2</sub>
<i>a</i> (Å)	11.544(6)	5.342(2)	9.279(7)	13.767(7)	6.053(3)
<i>b</i>	4.383(3)	10.028(4)	3.502(2)	5.414(3)	11.442(6)
<i>c</i>	3.574(2)	5.293(2)	6.731(6)	4.912(2)	8.330(3)
$\alpha$ (degr.)	90	90	90	81.42(4)	90
$\beta$	90	90	111.77(6)	81.42(4)	90
$\gamma$	90	90	90	130.33(4)	90
<i>V</i> (Å <sup>3</sup> )	180.8(2)	278.29	203.12	264.15	576.92
Space group	<i>Pmn</i> 2 <sub>1</sub>	<i>Cmc</i> 2 <sub>1</sub>	<i>C2/m</i>	<i>P</i> – 1	<i>Cmca</i>
Polyhedron around V	Dist. trig. bipyramide	Tetragon. pyramide	Dist. octahedron	Tetrahedron with addi- tional V ··· O inter- action	Dist. tetrahedron
V–O (Å)	1.578(7)–2.031(5), 2.805(7)	1.65(1)–1.92(1)	1.671(2)–2.111(3), 2.671(3)	1.629(3)–1.817(4), 2.440(4), 2.869(3)	1.695(1)–1.809(1)
V, O motives	Sheets IIac	Sheets IIac	Sheets IIab	Chains of V <sub>2</sub> O <sub>7</sub> groups IIa, chains form sheets in (001)	Sheets II [011]
Connection of V-polyhedra via Polyhedron around Mg	O ··· O edges O epixes [6 + 4], see text	O ··· O edges Pentagonal pyramide	O ··· O edges O epixes Octahedron	O ··· O edges in chains Octahedron	O epixes Octahedron
Mg–O (Å)	2.50(18)–2.58(24)	1.947(8)–2.07(1)	2.024(3)–2.199(2)	1.992(3)–2.246(4)	2.022(1)–2.138(1)
Mg, O motives	Chains II c	Chains	Chains II b	Chains, sheets O ··· O edges in chains, O epixes in sheets	Sheets II [011] O ··· O edges
Reference	This work	11	12	13	14

make a reliable suggestion about the coordination of the supposed Mg atom. Nevertheless, the coordination spheres around each Mg(1) atom may be described as [6 + 4] with six “shorter” (four Mg(1)–O(1) of 2.50(18) Å and two Mg(1)–O(3) of 2.57(24) Å) and four “longer” Mg ··· O distances (Mg(1) ··· O(2d) of 2.81(16) Å, Mg(1) ··· O(2a) of 3.26(17) Å and two Mg(1) ··· O(3) of 3.11(23) Å). Even the shortest Mg(1)–O distances in crystal I do exceed the Mg–O distances of 1.90–2.30 Å typically observed in Mg vanadates, where Mg has hexacoordination (Table 6). The effective ionic radius of Mg<sup>2+</sup> in the surrounding oxygen increases in the sequence 0.57–0.66–0.72–0.89 Å when its coordination number increases as 4–5–6–18 (15). As a first approximation, for the description of structure I with coordination of Mg [6 + 4], the effective ionic radius of 0.89 Å

should be taken for Mg with coordination number 8. Nevertheless, taking into account the essential weakness of the four additional Mg ··· O bonds, the surrounding oxygen coordination of Mg in crystal I should be considered as unsaturated.

The refinement of structure II in noncentrosymmetric and centrosymmetric space groups gave very similar values of the V–O separations (Table 7), which agree with those observed in the earlier studies (16, 17).

The observation of large Mg(1) ··· O separations in crystal I may be explained by a very small occupation factor of Mg(1),  $x = 0.011$ , i.e., by the necessity of the shift of positions of only around 1% of oxygen atoms from their positions in the original V<sub>2</sub>O<sub>5</sub> lattice. This means that the real Mg(1)–O separations in crystal I may be smaller than they appear from the X-ray single crystal results. The orientation of the thermal ellipsoids of oxygen atoms to the position of Mg(1) in crystal I may be an indirect confirmation of this explanation (Table 8). The coincidence, in fact, of the V–O separations in the structures of the product of Mg<sup>2+</sup> insertion (Table 5) and native single crystal II (Table 7) may be also explained by very small amount of inserted Mg<sup>2+</sup> cations.

Finally, the possibility of the existence of a Mg species in lattice I as more complicated ions such as Mg(OH)<sup>+</sup>

TABLE 7  
The V–O Separations (Å) in Structures IIa and IIb

	IIa	IIb		IIa	IIb
V(1)–O(1)	1.576(3)	1.583(3)	V(1)–O(2)	2.026(2)	2.026(2)
V(1)–O(2a)	1.865(2)	1.883(1)	V(1)–O(2b)	1.898(2)	1.883(1)
V(1)–O(3)	1.782(3)	1.781(1)	V(1) ··· O(1a)	2.803(3)	2.800(3)

TABLE 8  
Anisotropic Displacement Parameters ( $\text{\AA}^2 \times 10^3$ ) in  
Structure I

	$U_{11}$	$U_{22}$	$U_{33}$	$U_{12}$	$U_{13}$	$U_{23}$
V(1)	4(1)	23(1)	16(1)	-1(1)	0(1)	6(1)
O(1)	21(3)	21(3)	30(5)	-2(2)	-9(4)	23(5)
O(2)	7(2)	33(3)	15(3)	-3(2)	4(5)	-23(5)
O(3)	8(3)	28(4)	19(4)	0	0	11(8)

cannot be excluded, which leads to the increased Mg ··· O separations as well, when compared to the “normal” Mg, O compounds.

In the literature there are some discussions about the possibility of increased Mg ··· O separations. In the crystal of  $\alpha$ -Mg<sub>2</sub>P<sub>2</sub>O<sub>7</sub> a very distorted octahedron around one of two symmetrically independent Mg species can only be constructed by including a very long distance of 3.35 Å; other Mg–O distances at this species are 1.98–2.05 Å (18). But the coordination of this Mg species in  $\alpha$ -Mg<sub>2</sub>P<sub>2</sub>O<sub>7</sub> may be also described as a distorted square pyramid which shares two edges and one vertex with two neighboring octahedra and has a 3.35 Å nonbonded contact with a third octahedron (19).

The size of the unit cell of crystal I ( $V = 180.8(2) \text{\AA}^3$ ) is equal to that observed in structure II (180.7(1)  $\text{\AA}^3$ ). The first single crystal structure determination of V<sub>2</sub>O<sub>5</sub> (5) gave the value of unit cell volume by ca. 1% smaller (179.1  $\text{\AA}^3$ ). Our recent powder diffraction study (3) also gave a value which is ~0.5% smaller than that in I ( $a = 11.5204(9) \text{\AA}$ ,  $b = 3.5674(5) \text{\AA}$ ,  $c = 4.3780(4) \text{\AA}$ ,  $V = 179.93 \text{\AA}^3$ ).

In our opinion, the location of Mg on the suggested crystallographic positions Mg(1) of crystal I is not in contradiction with the known structural and electrochemical properties of V<sub>2</sub>O<sub>5</sub> crystals, exposed to the electrochemical Mg<sup>2+</sup> insertion. A more precise X-ray structure determination of the product of insertion of Mg<sup>2+</sup> in the V<sub>2</sub>O<sub>5</sub> single crystal failed because the attempts to treat the V<sub>2</sub>O<sub>5</sub> single crystals electrochemically for a prolonged time period (in order to insert more Mg<sup>2+</sup>) in the bulk destroyed the single crystallinity of the samples.

## CONCLUSION

The location of small amounts of Mg in the bulk V<sub>2</sub>O<sub>5</sub> structure is suggested. However, the majority of Mg is located on the surface of the V<sub>2</sub>O<sub>5</sub> crystals. The diffusion of Mg<sup>2+</sup> ions into the bulk of V<sub>2</sub>O<sub>5</sub> is slow and incomplete under the conditions expected in a real Mg battery. Therefore, the achievement of a high degree of bulk conversion (other words, a high charge density of V<sub>2</sub>O<sub>5</sub>-based electroactive materials) will be difficult.

## ACKNOWLEDGMENTS

The authors are very indebted to Professor K. Kato (National Institute for Research in Inorganic Materials, Tsukuba, Japan) for the gift of the V<sub>2</sub>O<sub>5</sub> single crystals, W. Scheifele (PSI) for technical assistance, and Dr. O. Haas (PSI) for many fruitful discussions. We also thank the Swiss Federal Energy Office for financial support (Grants EF-REN(91)054 and EF-PROCC(91)18).

## REFERENCES

1. P. Novák and J. Desilvestro, *J. Electrochem. Soc.* **140**, 140 (1993).
2. P. Novák, W. Scheifele, and O. Haas, *Molten Salt Forum* **1–2**, 389 (1993/1994).
3. P. Novák, V. Shklover, and R. Nesper, *Z. Phys. Chem.* **185**, 51 (1994).
4. K. Kato, personal communication.
5. “CAD4-EXPRESS. User Manual.” Delft Instruments X-ray Diffraction, Delft, 1992.
6. G. M. Sheldrick, “SHELXTL-PLUS, Crystallographic System, Version 2.” Nicolet XRD Corp., Madison, WI, 1988.
7. “Digital Micrograph. Users Guide, 1992–1994.” Gatan, Inc., 6678 Owens Drive, Pleasonton, CA.
8. V. Shklover and T. V. Timofeeva, *Russ. Chem. Rev.* **54**, 1057 (1985).
9. V. Shklover, T. V. Timofeeva, and Yu. T. Struchkov, *Russ. Chem. Rev.* **55**, 721 (1986).
10. C. Delmas, in “Lithium Batteries. New Materials, Developments and Perspectives” (G. Pistoia, Ed.), p. 468. Elsevier, Amsterdam, 1994.
11. J.-C. Bouloux, I. Milosevic, and J. Galy, *J. Solid State Chem.* **16**, 393 (1976).
12. H. N. Ng and C. Calvo, *Can. J. Chem.* **50**, 3619 (1972).
13. R. Gopal and C. Calvo, *Acta Crystallogr. Sect. B* **30**, 2491 (1974).
14. N. Krishnamacher and C. Calvo, *Can. J. Chem.* **49**, 1629 (1971).
15. R. D. Shannon, *Acta Crystallogr. Sect. A* **32**, 751 (1976).
16. H. G. Bachmann, F. R. Ahmed, and W. H. Barnes, *Z. F. Kristallogr.* **115**, 110 (1961).
17. R. Enjalbert and J. Galy, *Acta Crystallogr. Sect. C* **42**, 1467 (1986).
18. C. Calvo, *Acta Crystallogr.* **23**, 289 (1967).
19. M. Souhassou, C. Lecomte, and R. H. Blessing, *Acta Crystallogr. Sect. B* **48**, 370 (1992).